

Role of Cyclooxygenase-2 in neural crest cell delamination and migration during early embryogenesis in the chick

INTRODUCTION

Embryonic development involves intricate coordination of molecular, cellular, and tissue-level processes that must occur according to strict schedules of time and location. Amongst which, craniofacial complex represents one of the most highly diversified and evolutionarily adapted anatomical aspects of vertebrates. Craniofacial development is a unique and complex process that begins once the anterior–posterior axis of the embryo is established at the same time the major contributor of craniofacial patterning arises, that is, neural crest cells, and involves the interaction of diverse cell populations (Baker & Bronner, 1997; Trainor, 2005; Fish, 2016). In 1868, While His described a structure in the ectoderm whose cells are formed at a distance, and he named this as ‘Zwischen’ strand; this brought the novel realization that cells in a tissue are not necessarily stationary (His, 1868). The strand of Zwischen is nothing but neural crest cells. The emergence of neural crest cells is a pivotal event of animal evolution which leads to the formation of the jaw, face, skull, and bilateral sensory ganglia of vertebrates (Northeutt & Gans, 1983). Neural crest cells are derived from the ectoderm, but due to their ability to form various structures during organism development, it has been called the ‘fourth germ layer’ (Hall, 2018). These cells are strictly vertebrate elements, but their genes and gene regulatory network are present even in non-vertebrate chordates as well (Yu et al., 2008).

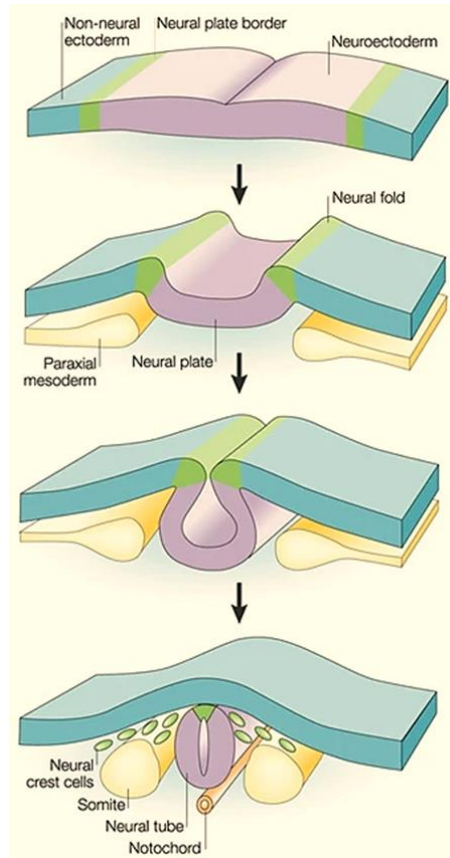


Figure 3.1: Emergence of neural crest cells from the neural tube, neural plate border (green) which after neurulation become the neural crest cells that delaminate from the dorsal side of the neural tube (Gammill & Bronner, 2003)

The neural crest cells originate as a result of a chain of interactions beginning at the time of gastrulation from the dorsal ridge of the neural tube. Specifying the neural crest at the neural plate epidermis boundary is a multistep process (Huang and Saint-Jeannet, 2004; Meulemans and Bronner-Fraser, 2004). The first step appears to be the specification of the neural plate border (Fig 3.1). The cells in this border between the neural plate and the epidermis will become the neural crest, and (in the anterior region) the placode thickenings in the surface ectoderm will generate the eye lens, inner ear, olfactory epithelium, and other sensory structures. Neural crest cells exist along the entire axial length of the neural tube at the most rostral forebrain and give rise to many types of cells, such as neurons, epinephrine-producing cells, pigment cells of the epidermis, and many connective tissue components of the head (Le Douarin et al., 1993; Creuzet et al., 2005). Based on the structures formed by neural crest cells and the origin from the neural tube region, there are four different types of neural crest cells: Cranial neural crest (CNC), Trunk neural crest, sacral neural crest cells and Vagal neural crest cells (Le Douarin & Kalcheim, 1999). All four types overlap with each other during the formative phase of development (Fig 3.2).

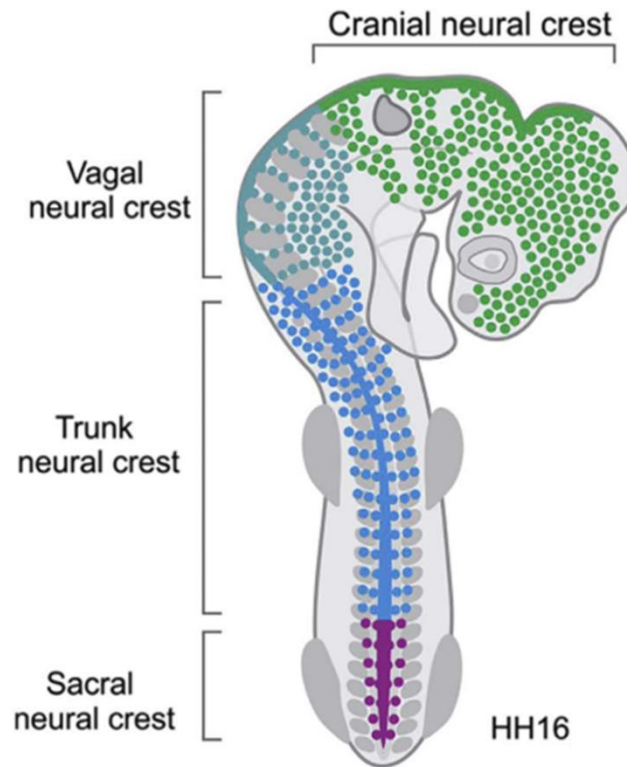


Figure 3.2: Overview of the distribution of neural crest subpopulations along the anterior-posterior axis on HH16 developmental stage of chick embryo (Rothstein et al., 2018)

Cranial neural crest cells (CNCCs)

Cranial neural crest cells emerge from the hindbrain (rhombomere 1-7) and are spatially distributed along discrete migratory pathways. They produce craniofacial mesenchyme, which differentiates into cartilage, bone, cranial neurons, glia, and pigmented cells of the face (Graham et al., 2004; Cordero et al., 2011). CNCCs also migrate to pharyngeal arches and pouches to give rise to thymic cells, odontoblast of tooth primordia, middle ear, and jaw bones (Parada et al., 2012).

Cardiac neural crest cells

Cardiac neural crest cells are a subpopulation of cranial neural crest cells. They are necessary for normal cardiovascular development. The cardiac neural crest cells originate from the dorsal neural tube between the mid-optic placode lasting till the posterior border of the third somite. The cardiac neural crest cells are required for the re-patterning of the heart tube and smooth muscle of arteries (Bockman et al., 1989; Bergwerff et al., 1998). These cells also form the muscular connective tissue wall of large arteries (the outflow

tract) and separate pulmonary circulation from the aorta (Le Lievre & Le Douarin, 1975; Sizarov et al., 2012).

Trunk neural crest cells

Trunk neural crest cells show a transient appearance; they disappear soon after neural tube closure. They migrate through two major routes, ventrolateral (anterior half of each somatic sclerotome) and dorsolateral route. Through the ventrolateral route trunk, neural crest cells remain in the sclerotome and form dorsal root ganglia containing sensory neurons. The other route of migration is dorsolateral, through which cells migrate in the dermis of the skin and produce precursors of melanocytes (Gammill & Roffers, 2010).

Vagal and Sacral neural crest cells

The vagal and sacral neural crest overlaps the cranial and trunk neural crest lying opposite to somite, 1-7 while the sacral neural crest lies posterior to somite 28 (Douarin & Teillet, 1973; Pomeranz et al., 1991). The vagal neural crest contributes to the formation of the enteric nervous system. In chick embryos, a subpopulation of vagal neural crest takes the ventral path between the neural tube and dermomyotome, eventually giving rise to sensory ganglia, sympathetic ganglia, or enteric ganglia (Reedy et al., 1998). The vagal neural crest cells from the rostralmost region migrate to the vagus nerve and invade the foregut of the mouse embryo (Espinosa-Medina et al., 2017).

A sacral neural crest is a distinct group of cells that migrate along a definite pathway from the neural tube to the hindgut. They exhibit a discrete migratory behaviour within gut mesenchyme and form neurons and glial cells of the hindgut enteric system (Wang et al., 2011).

Among all the different types of neural crest cells, cranial neural crest cells play a major role in the development of craniofacial structures as their stemness allows them to differentiate into various tissue types during the development of the embryo.

Cranial neural crest cells and facial development

Cranial neural crest cells form connective tissue, cartilage, and bone of the craniofacial region, including most of the head skeleton (Fig 3.3). There are many congenital craniofacial defects that occur due to alterations in CNCC delamination, migration, and differentiation. Multiple different animal models were used to study the cranial neural crest

cells in vertebrate facial patterning and one of the widely used animal models is the chick embryo, due to the benefits of its external development and similarity in the migration pattern of cells (Johnston, 1966; Santagati & Rijli, 2003; Tatarakis et al., 2021).

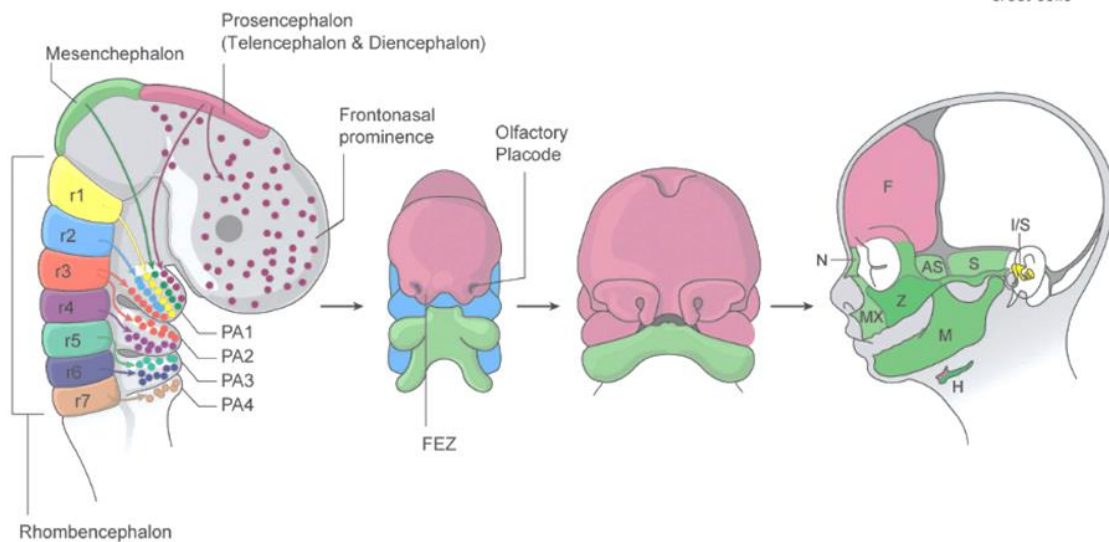


Figure 3.3: Cranial neural crest cells exhibit patterns of migration and differentiation into bone and cartilage of craniofacial region (Fitriasari & Trainor, 2021)

The three different signaling sources interact with the neural plate and epidermis and lead to CNCC induction. Specification of CNCC occurs during gastrulation, but it depends upon signaling; Wnt activation and BMP inhibition from the dorsolateral mesoderm (Steventon et al., 2009). During neurulation, when neural folds join and form the neural tube, the CNCC present in the dorsal ridge of neural tube delaminate. Five different families of extracellular inductive molecules have been found to be involved in neural crest cells induction: Wnts, BMPs, FGFs, RA, and Notch/Delta (Villanueva et al., 2002; Cornell & Eisen, 2005; Steventon & Mayor, 2012; Shi et al., 2011). During delamination CNCCs move collectively as a cohesive population and undergo a progressive dissociation into smaller clusters which then separate as individual cells as their migration progresses (Bronner, 1993; Theveneau & Mayor, 2012). Along with that, *Msx*, *Dlx*, *Pax3*, and *Pax7* are neural plate border specifier genes, and their expression patterns correlate with the ventral-dorsal gradient of BMP (Monsoro-Burq et al., 2005; Milet & Monsoro-Burq, 2012). The crest cells which arise from the hindbrain migrate in three distinct streams adjacent to rhombomeres 2, 4, and 6 and followed to populate in the first, second, and third branchial arches (Lumsden et al., 1991; Ellies et al., 2002). In branchial arches, the CNCC interact with facial epithelium and neuroectoderm and contributes to facial prominence formation, which eventually forms various structures.

Independent of the timing of CNCC specification, contact-mediated signaling between the tissues in the dorsal tube results in neural ectoderm cells and non-neuroectoderm border formation. These non-neuronal ectodermal cells undergo EMT, and forms CNCC which migrate to various regions of developing embryo. Delamination is a collective effort orchestrated by downstream targets of Wnt3A and BMP4 signalling. EMT is a multistep process required for the migration of CNCC, where the cells lose apicobasal polarity and disable the intracellular adhesions (Acloque et al., 2009). In terms of neural crest delamination and migration, cadherins play an essential role; cells decrease the E-cadherin expression and elevate N-cadherin expression. The entire process of cadherin switching is initiated by zinc finger like transcription factors Snail1 and Slug (Snail2) (Nieto et al., 1994; Cano & Nieto, 2008). Snail represses E-cadherin through histone deacetylase-mediated chromatin remodelling (Peinado et al., 2004). The slug marker of NCCs is involved in migration, and it functions via the upregulation of RhoB, which regulates actin organization and membrane trafficking (Prendergast, 2001). Migratory CNCC follows stereotypic routes for craniofacial development. These pathways are very well conserved across the species. CNCCs migrate using the local extracellular matrix available to them. The ability of cells to use these matrices for migration depends on the expression of specific transmembrane receptors for each of these matrix components. Members of FGF and PDGF families as well as VEGFA, Sdf1 are all positive regulators of neural crest migration and have been proposed as chemo-attractants (Belmadani et al., 2005; Kulesa et al., 2010; Svetic et al., 2007).

The canonical Wnt/ β -catenin signaling pathway is reported to play a significant role in the formation and progression of CNCCs, as it influences both delamination and migration by interacting with *BMP4* and *TGF- β* , respectively (Abu-Elmagd et al., 2006; Duband, 2006). One important molecule among the numerous regulatory elements that have been linked to delamination and migration is COX-2, an induced isoform of cyclooxygenase that catalyzes the synthesis of PGE₂ from arachidonic acid (Ricciotti & FitzGerald, 2011). COX-2 mediated PGE₂ synthesis modulates a multitude of signal transduction pathways such as Wnt/ β -catenin, BMP, and TGF- β to play a crucial role in cellular events, including cell proliferation, migration, EMT, and differentiation (Buchanan et al., 2003, Abrahao et al., 2010). Jang and colleagues (2009) found that COX-2 primarily induces EMT in colon cancer cells by altering E-cadherin expression in mice (Jang et al., 2009). COX-2 is known

to control cancer cell metastasis by interacting with TGF- β and its downstream targets (Neil et al., 2008).

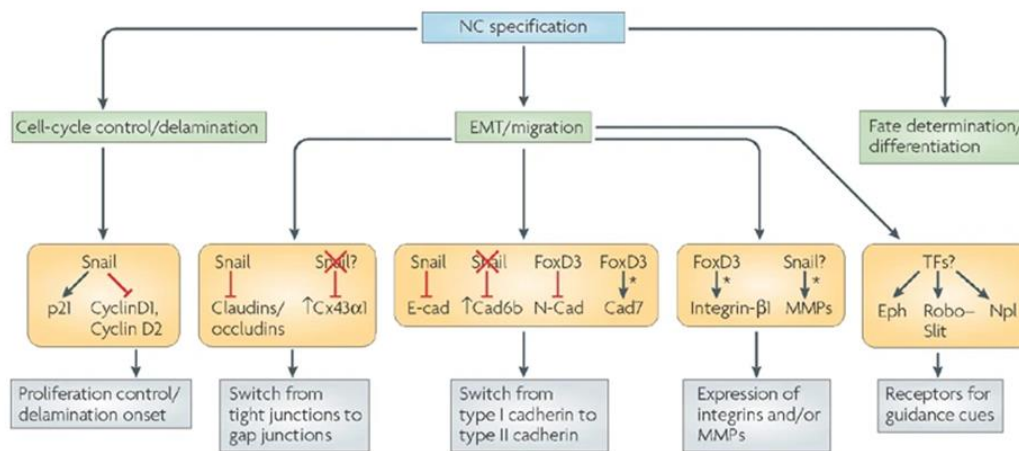


Figure 3.4: Signaling pathway regulating specification and migration of neural crest cells (Sauka & Bronner, 2008)

Previous studies in the lab using chick embryo indicates that the absence of COX-2 activity cause defects in vascularization, tissue integrity, and limb (Verma et al., 2021). Among all developmental defects, craniofacial anomalies are the most prevalent congenital anomalies. In this study, it was also observed that selective inhibition of COX-2 reduced only the concentration of PGE₂, while the concentrations of the other prostanoids remained unchanged. Based on these findings and the reported potential interactions of COX-2 with various signaling molecules, we hypothesized that the pathways regulating CNCC delamination and migration might be altered by COX-2 inhibition, leading to craniofacial defects in developing embryos. In the present study, the activity of COX-2 was inhibited using etoricoxib, a selective COX-2 inhibitor, and the effect of this on the regulators of CNCC migration and neural tube closure in chicken embryos was determined.

MATERIALS & METHODS

The aim of this chapter was to elucidate the role of COX-2 in neural crest cell delamination and migration using chick embryos. To understand the delamination and migration of the neural crest cells, initial developmental stages such as HH6, HH12, and HH20 were considered for the study. At HH6, the neural folds start joining each other, and from the dorsal ridge, the neural crest cells start delaminating, followed by HH12 when the cells

start migrating to the dorsal or ventral side of the neural tube, and on HH20, neural crest cells migrate towards the pharyngeal arches.

The collected eggs were cleaned with betadine and divided into two groups - control and etoricoxib treatment. The treatment was carried out using the air sac method as described in the methodology section (Chapter 2) of the thesis. The embryos of desired developmental stages were collected at 24hrs (HH6), 48hrs (HH12), and 72hrs (HH20) after incubation at 37°C. While collecting embryos from both groups, mortality was noted. The etoricoxib inhibits COX-2 and is incorporated into the developing embryo, which was checked through LC-MS/MS analysis of different stages of developing embryos (Verma et al., 2021). The COX activity assay was performed in both groups of embryos to check the inhibition in the activity of COX-2 by etoricoxib. The morphological observation was made in the control and treated groups of the embryos to identify the defects due to COX-2 inhibition. Further, to understand the effects of COX-2 inhibition at the molecular level, transcripts and protein levels of migratory and delaminating molecules were analyzed using q-RT PCR and western blot. H & E staining for HH12 sections was carried out to observe the CNCC migration in both groups of embryos.

RESULTS

Mortality and COX activity

The dose of 0.07mg/ml was injected into an air sac of freshly laid eggs, and COX-2 activity assay was performed, which showed a significant decrease in the activity of COX-2 in etoricoxib-treated embryos as compared to control embryos of HH6, HH12, and HH20 (Fig 3.5, Table 3.1). Further, COX-2 inhibition led to a marginal but statistically significant increase in embryonic mortality at all stages examined. As a result, 50 eggs were incubated for each group in order to ensure that at least 30 embryos survived the experiment.

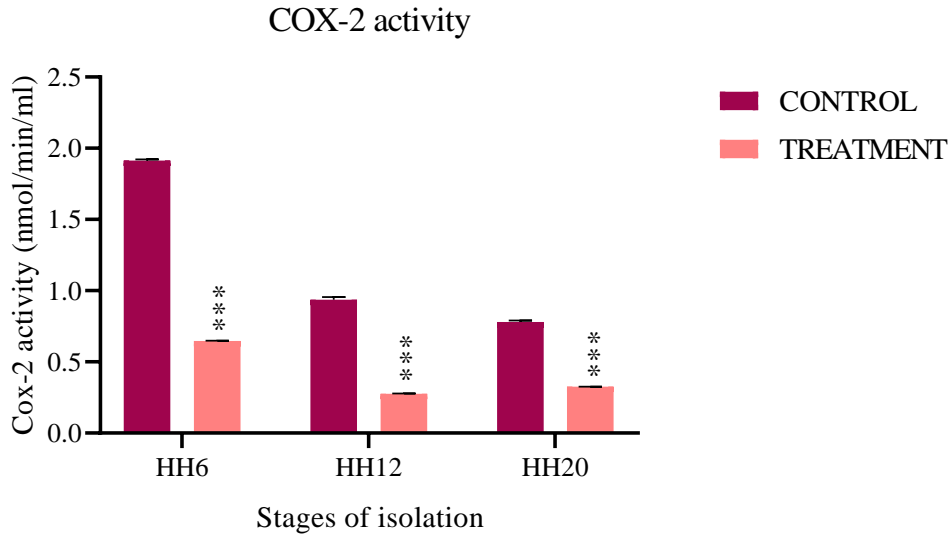


Figure 3.5: COX-2 activity estimated in control and treated embryos isolated at HH6, HH12 and HH20 of development; *** $p \leq 0.001$

Prostaglandin E₂ is a product of the active COX-2 enzyme. Levels of PGE₂ were analyzed in the control and treatment group of embryos at HH6, HH12, and HH20. A decrease in PGE₂ level was observed in the treatment group of embryos when compared to the control embryos of the same stage (Fig 3.6, Table 3.1).

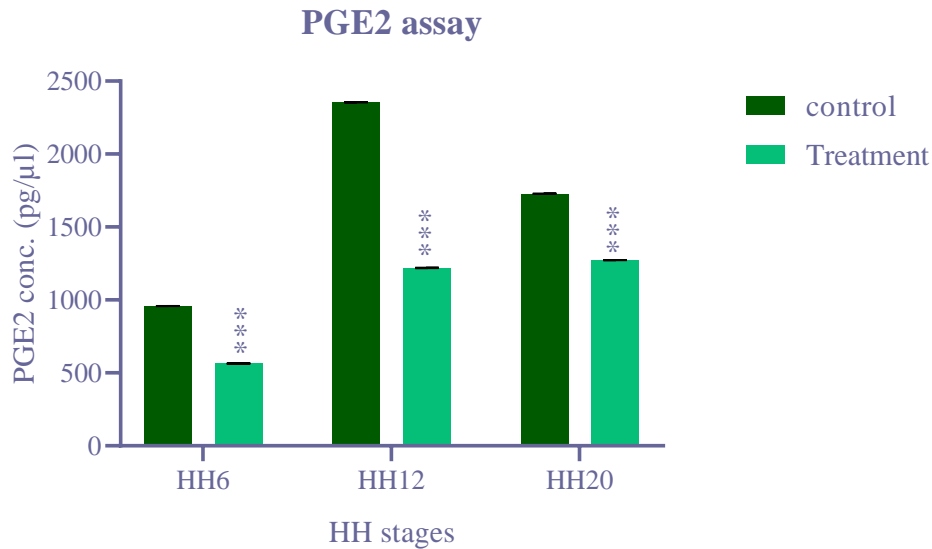


Figure 3.6: PGE₂ estimation in HH6, HH12, and HH20 control and treatment group of embryos; *** $p \leq 0.001$

Mortality Analysis

The embryos of control and treatment groups were analyzed for mortality. The analysis indicates HH6 stage control has a lower mortality rate than the etoricoxib-treated embryos. As the developmental process progresses, the mortality increases in the HH12 and HH20 stage treatment group of embryos as compared to control embryos (Table 3.2).

Morphological defects and analysis

The presence of COX-2 from the very first day of chick development points to its possible regulatory role in embryogenesis. To further assess this role, the activity of COX-2 was inhibited by using the pharmacological inhibitor etoricoxib. The embryos treated with etoricoxib showed disrupted neural folds; the neural tube remained distorted and incompletely formed neural tube in the HH6 stage (Fig 3.7B-C). Whereas the HH6 control group of embryos showed proper neural fold closing and neural tube formation (Fig 3.7A).

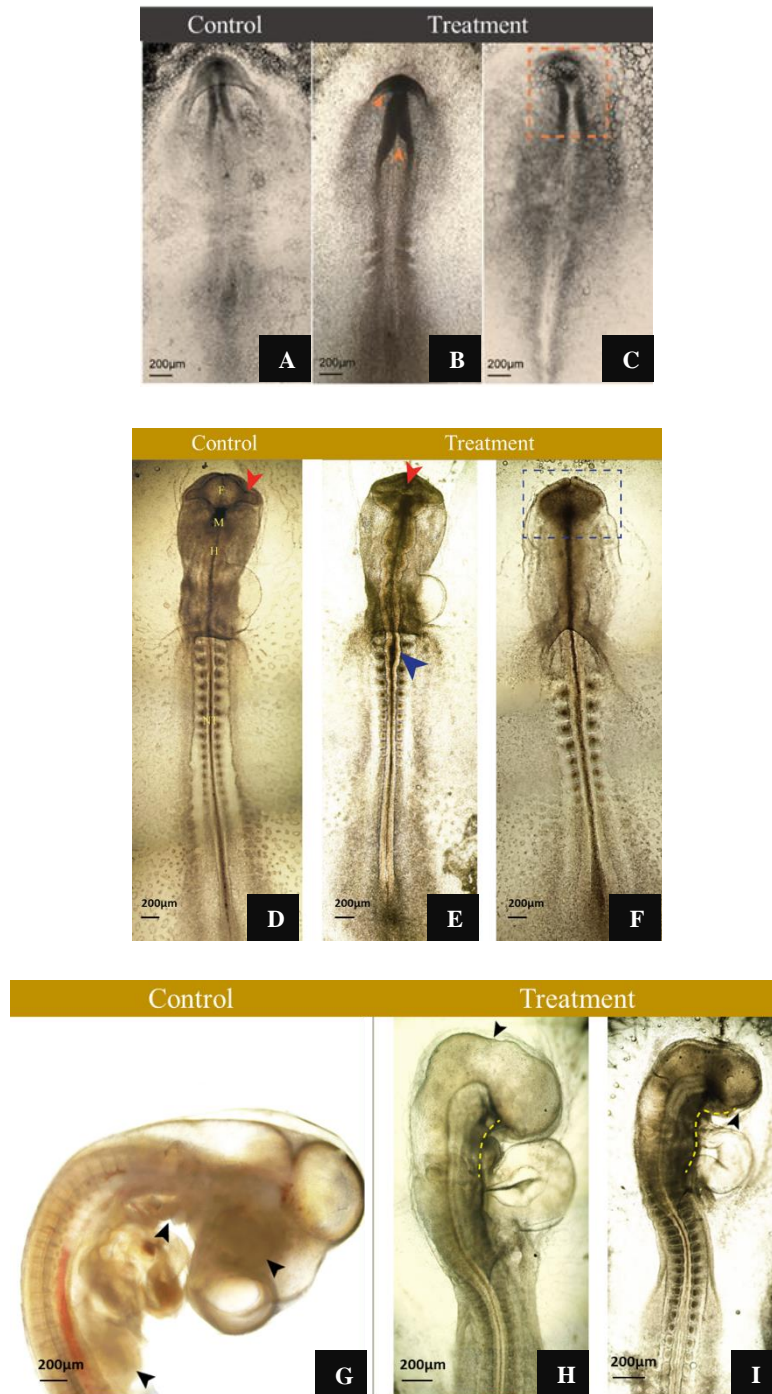


Figure 3.7: Morphological aberrations due to COX-2 inhibition in HH6, HH12, and HH20 stages. (A) Control embryo at HH6 stage with well-developed neural folds aligned at the center; (B-C) Etoricoxib treated embryos at HH6 developmental stage with defective neural fold (orange arrowhead & dotted box); (D) Control embryo at HH12 stage with defined optic vesicles (red arrowhead) and brain vesicles; (E-F) HH12 stage embryo of treatment group with incomplete brain vesicles (red arrowhead), open neural tube region (blue arrowhead) and defective optic vesicle (blue dotted box); (G) HH20 stage control embryo with distinct three brain regions, eye, pharyngeal arches, limb bud (black arrowhead); (H-I) HH20 stage Etoricoxib treated embryos with abnormal pharyngeal arch (yellow dotted line), delayed brain formation and optic cup poorly developed (black arrowhead)

The control group of HH12 stage embryos has defined rhombomeres, a compact neural tube, an optic vesicle, and an optic stalk (Fig 3.7D). However, the treated embryos displayed improper closure of the neural tube, a reduced number of somites, distorted rhombomeres, absence of single or both optic stalks along with the overall delayed development of craniofacial structures (Fig 3.7E-F). Further, on HH20 treatment group of embryos have abnormal cervical flexure, absence of single or both optic cups, defective optic cup, and abnormal pharyngeal arches or absence of pharyngeal arches (Fig 3.7H-I) as compared to control embryos of the same stage (Fig 3.7G).

Gene expression analysis

Treatment of etoricoxib and morphological defects were linked by analyses of delamination and migratory genes. Numerous genes are checked for their presence and modulation in the experimental group compared to control embryos.

As mentioned previously, Wnt/ β -catenin and TGF- β , along with their downstream molecules, play a significant role in EMT, cell survival, and proliferation during CNCC migration. As a result, the transcriptional status of *WNT3A*, *TGFB*, *MSX1*, *TWIST*, *CDH1*, *CDH2*, *VIM*, and *CASP3* was investigated throughout all three stages in both groups. Compared to the control, treated embryos showed a significant decrease in the level of *WNT3A* expression on HH6, while only a marginal decline occurred in the level of TGF- β transcripts. In the meantime, *MSX1* demonstrated a remarkable increase that was ten times higher in the treated embryos. Similarly, the treatment group of embryos had a negligible increase in *TWIST* transcripts and a noticeable increase in *CDH1* gene expression on HH6 as compared to control embryos. There was a noticeable reduction in *CDH2* and *VIM* gene expression in COX-2 inhibited group of embryos on HH6. Along with that, *PCNA* and *CASP3* decreased significantly in the treatment group of the embryo as compared to the control (Fig 3.8A, Table 3.3).

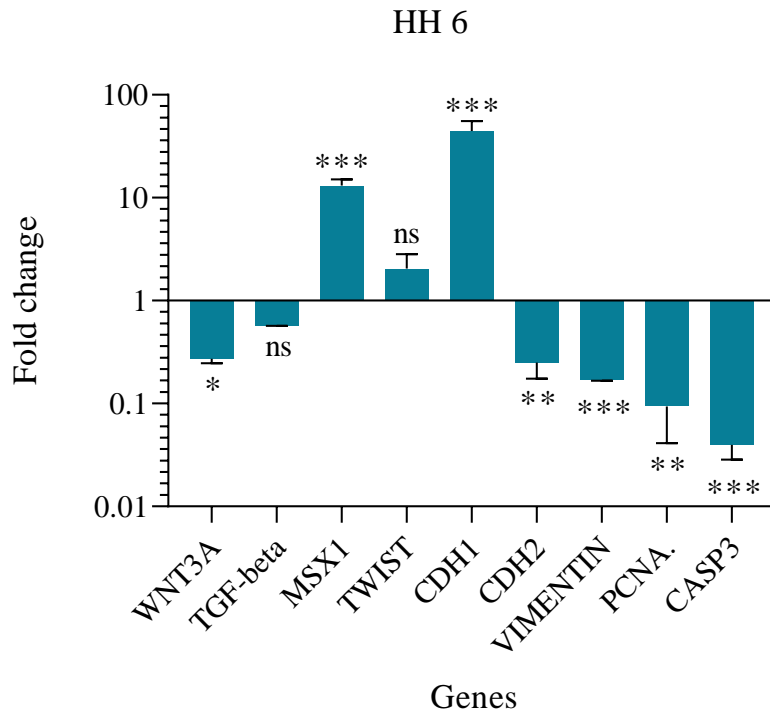


Figure 3.8 A

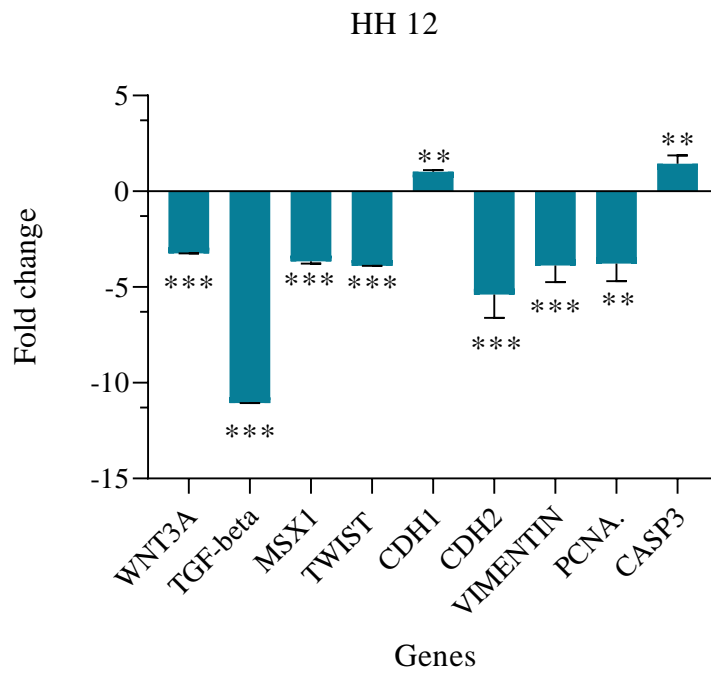


Figure 3.8 B

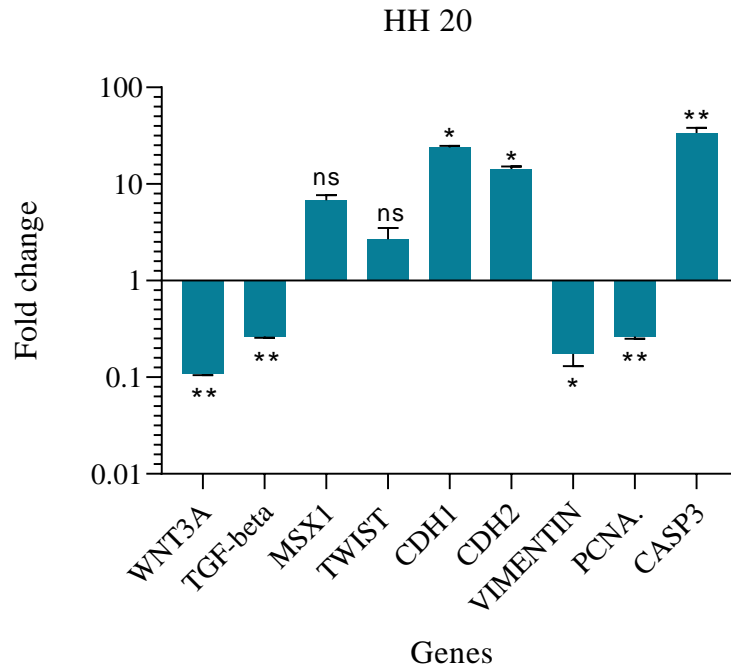


Figure 3.8 C

Figure 3.8 A-C: Gene expression analysis of genes responsible for CNCC migration on HH6 (A), HH12 (B), and HH20 (C) stages of chick embryo. Each gene expression of treatment group of tissue is compared with control group of tissue and represented as fold change; ns=non significant; * $p \leq 0.05$; ** $p \leq 0.01$; *** $p \leq 0.001$.

On HH12, etoricoxib treated embryos showed reduced expression of *WNT3A*, *TGF- β* , *MSX1*, *TWIST*, *CDH2*, and *VIM*, whereas *CDH1* and *CASP3* transcripts increased significantly (Fig 3.8B, Table 3.4). Furthermore, on HH20, the transcript levels of *WNT3A*, *TGF- β* , *VIM*, and *PCNA* decreased significantly, along with *MSX1* and *TWIST* marginally increased in the treatment group of embryos (Fig 3.8C, Table 3.5).

Protein expression pattern in CNCC

The protein expression of regulatory molecules of CNCC delamination, proliferation, and migration, including E-cadherin, N-cadherin, FoxD3, Vimentin, PCNA, cleaved Caspase-3, and Sox2, was measured using western blot, followed by densitometric analysis of the bands.

The findings showed that E-cadherin was significantly upregulated in the treated embryos compared to the corresponding control embryos across all three stages examined (Fig 3.9). The levels of N-cadherin decreased significantly on HH6 in the treated group of embryos. A similar kind of trend was observed in HH12 and HH20 embryos. On HH6, the expression of FoxD3 protein was not found in either the control embryos or the treated embryos;

however, on HH12, the expression was significantly lower in the treatment group. In addition, compared to the control embryos, the level of FoxD3 continued to be low in the treated embryos on HH20 (Fig 3.9, Table 3.6).

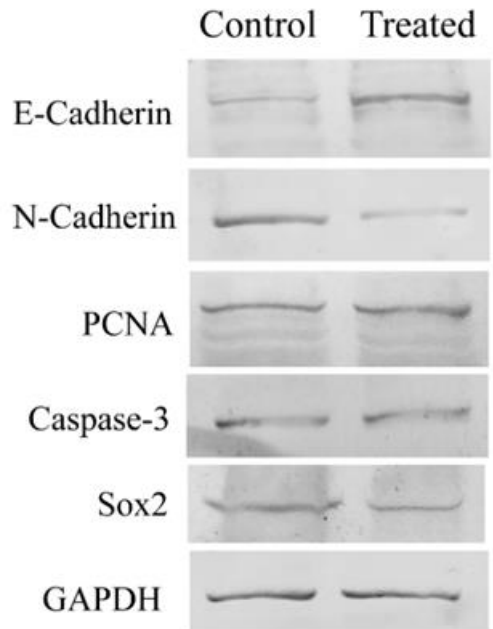


Figure 3.9: Expression of delamination and migration-specific proteins on HH6 stage of development in control and treated embryos

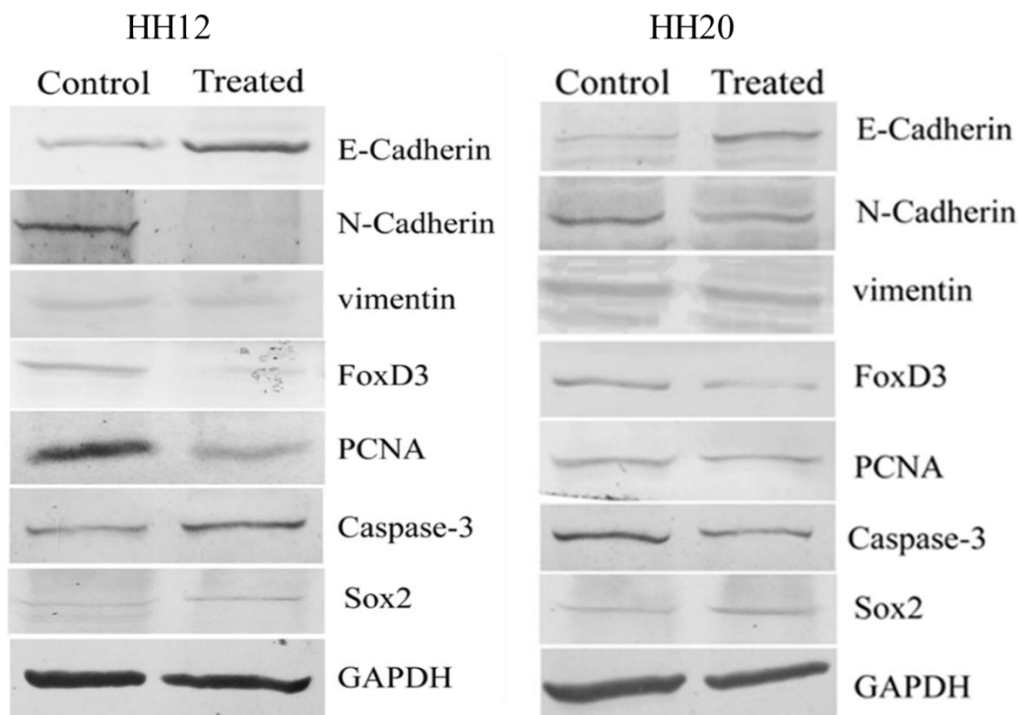


Figure 3.10: Protein expression pattern of delamination and migration-specific proteins on HH12 and HH20 development stages in control and treated group of embryos

Another crucial EMT regulator, namely Vimentin, was not recorded in the control and treated group of embryos on HH6. In contrast, on HH12, treated embryos showed no visible alteration compared to the respective control group (Fig 3.10, Table 3.6). However, on HH20, treated embryos showed a decrease in Vimentin expression compared to the control group. The results of a parallel analysis of PCNA showed that the expression of this gene did not change on HH6 compared to the control (Fig 3.9, Table 3.6), and then it declined significantly at the following stages (HH12 and HH20) (Fig 3.10, Table 3.6). Cleaved Caspase 3, on the other hand, showed decreased levels on HH6 in the treated embryos, while its level showed a significant increase in HH12 compared to the controls. On HH20, its level had increased, but not significantly, compared to the control group. In addition, when compared with the respective controls, the treated group of embryos exhibited lower levels of Sox2 on HH6, as well as on HH12 and HH20, respectively.

Immunohistochemistry

Considering abnormalities associated with CNCC production and migration, it was of interest to examine the locations of COX-2 protein in various regions of HH6 and HH12 stage embryos by immunostaining freshly sectioned tissues. Immunolocalization showed the presence of COX-2 in the periphery of neural tube cells in all three stages (HH6, HH12 and HH20) of control embryos. Along with neural tube cells, COX-2 shows faint expression in peripheral cells as well (Fig 3.11).

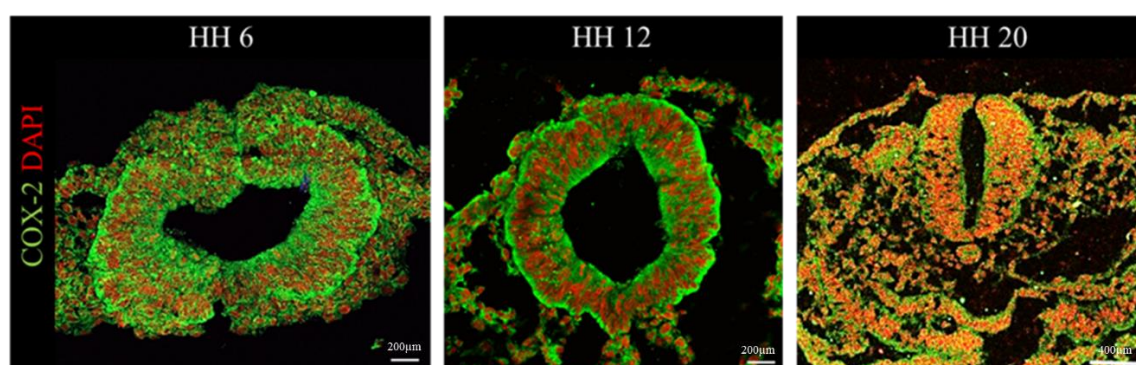


Figure 3.11: Immunolocalization to show the presence of COX-2 in HH6, HH12, and HH20 stages of development in control group of embryos

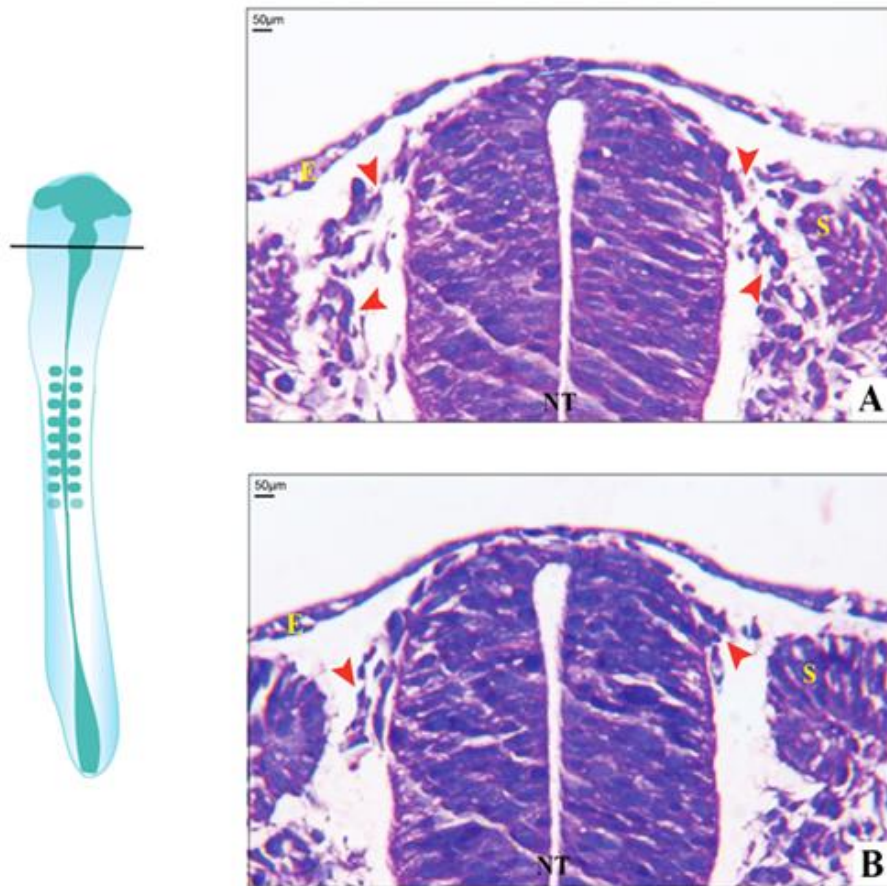


Figure 3.12: Histology of HH12 stage embryos. (A) Control embryo of HH12 stage with distinct neural crest cells around the neural tube (red arrowhead); (B) Etoricoxib treated embryos of HH12 stage with few neural crest cells around the neural tube (red arrowhead); E=epithelium, NT=neural tube, S=somites

Further on HH12, tissue sections of the control and treatment group of embryos were stained with Haematoxylin and Eosin (H&E), which revealed that control embryos have migrating CNCCs besides the neural tube, whereas in the case of etoricoxib treated embryos have a significantly lesser number of migrating CNCCs besides the neural tube (Fig 3.12).

DISCUSSION

Cranial neural crest cells are the most important source of progenitors and migrate to generate diverse facial features in growing embryos, including the frontonasal, maxillary, and mandibular prominences (Cordero et al., 2011). It has been determined that the avian model is ideal for understanding the mechanism of CNCC formation and migration, which is crucial for craniofacial development. It is closely related to mammals, and the migration

pattern of CNCCs are identical in both these groups of chordates as it remains conserved throughout evolution (Helms et al., 2005; Kiecker, 2016). It is widely recognized that the factors responsible for CNCC migration are conserved among various classes of vertebrates. One example of this type of factor is COX-2, which is a member of the cyclooxygenase family and has a role in multiple cellular processes, including proliferation, migration, angiogenesis, and differentiation (Evans et al., 1993; Wu et al., 2006; Sobolewski et al., 2010).

The inhibition of COX-2 by etoricoxib hampered CNCC delamination, migration, and survival, resulting in downstream morphological defects such as improper neural folds, defective head formation, or the absence of optic vesicles. Owing to abnormal CNCC migration or inadequate CNCC population, the current study focused on the expression patterns of signaling molecules that contribute to craniofacial patterning by determining the fate of CNCCs. COX-2 activity assay was performed to verify etoricoxib mediated inhibition of COX-2 in HH6, HH12, and HH20 stages of developing embryos. In fact, COX-2 is known to be localized in the neural tube region of developing chick embryos between developmental stages HH6 to HH20. In the present study, a reduction in COX-2 activity altered the levels of major regulators of the CNCC migration pathways in embryos of the treatment group. Under COX-2 inhibition, the expression of *TGF- β* and *Wnt3A*, as well as their downstream signaling factors *TWIST*, *MSX1*, *Sox2*, *FoxD3*, *Vimentin*, *CDH1*, and *CDH2*, were found to be altered. During the early embryogenesis of chicks, the involvement of *Wnt3A* in the delamination of CNCC has been recorded (Chalpe et al., 2010). COX-2 inhibition resulted in a significant decrease in the expression of *WNT3A* in the current study. Compared to the respective controls, its mRNA level decreased on HH6 and continued to decline on HH12 and HH20 in etoricoxib-treated embryos. A decreased *Wnt3A* levels caused a lower number of CNCCs formation. It was clearly observed in the histological study that the HH12 stage embryo exhibited CNCCs had disoriented and lesser in number compared to the control. Therefore, proving the impact of reduced COX-2 activity on normal CNCC formation and migration during early development through Wnt signaling.

Wnt3A and *TGF- β* are known to be involved in the process of delamination of CNCCs by EMT (Kalcheim & Burstyn-Cohen, 2003). In this study, *Wnt3A*, along with *TGF- β* , showed an unstable trend in all three developmental stages in the treated embryos. According to Sela-Donofeld and Kalcheim, a change in TGF-beta disrupts the migration pattern because

it is essential for the switching of cadherins during CNCC delamination (Sela-Donenfeld & Kalcheim, 2000). *MSX1* and *TWIST*, which are downstream mediators of *TGF- β* and *Wnt3A*, exhibited altered gene expression at all stages (HH6, HH12, and HH20) in the etoricoxib treatment group. *MSX1* is one of the downstream regulators that control early embryonic cell proliferation and differentiation. It is highly expressed in CNCCs and plays a crucial role in embryonic development in regulating the EMT process (Ishii et al., 2005). In the current results, a significant increase in *MSX1* gene expression on HH6 was followed by a gradual decrease in HH12 and HH20, substantiating the histological outcomes. CNCCs delamination was seen on HH6, but elevated *MSX1* expression impacts cell survival in decreased COX-2 activity. In normal conditions, CNCCs reside in pharyngeal arches when levels of *TWIST* decrease and acquire their fates. In this study, the level of *TWIST* remains high even at later stages (until HH20) under inhibition of COX-2. This hampers the ability of CNCCs to proliferate and differentiate into well-organized cranial features.

It is well established that during CNCC formation, epithelial cells undergo mesenchymal fate through EMT. During EMT, E-cadherin is downregulated, leading to negative impacts on cell-cell adhesion. This results in cytoskeletal changes, allowing for cell motility (Rogers et al., 2013). EMT is a process well regulated by levels of E-cadherin, N-cadherin, and Vimentin. The decline in CDH1 and escalation in CDH2 levels leads to the initiation of EMT in the dorsal ridge of the neural tube to generate neural crest cells (Taneyhill, 2008). In the present study, embryos with compromised COX-2 activity exhibited increased E-cadherin at gene and protein levels. This was followed by a decrease in vimentin and N-cadherin on HH6 and HH12, which hindered CNCC formation and migration. However, by HH20, CDH1 and CDH2 had returned to similar levels, apparently due to the embryo's compensatory nature or feedback mechanism (Pla et al., 2001; Hovland et al., 2020). Even on HH20, the transcript and protein levels of vimentin remained low, indicating an abnormal EMT. This altered the patterning of the head, optic vesicle, and neural tube in the embryo treated with etoricoxib.

Additionally, the expression of *FoxD3*, a crucial pre-migratory and migratory CNCCs marker, was evaluated (Stewart et al., 2006). *FoxD3* regulates the expression of cell adhesion molecules, such as E-cadherin and N-cadherin, during neural crest formation in mice (Cheung et al., 2005). In the present study, its protein expression was measured beginning on the HH12 stage in both the control and treatment groups. This

supports the fact that FoxD3 expression in developing chick embryos does not begin until the HH8 stage (Kos et al., 2001). FoxD3 protein expression in treated embryos decreased in HH12 and HH20 stages relative to the respective controls. This indicates that COX-2 inhibition has detrimental effects on the CNCC population and its migration.

In order to comment on the cell proliferation in CNCCs, the *PCNA* transcript and protein level were measured and found to be significantly lower in treated embryos on all three stages compared to control embryos. In accordance with these findings, cleaved Caspase-3 gene and protein expression were significantly upregulated at all three stages in the treatment group. These results suggest the aberrant cell proliferation of delaminated CNCC, due to the absence of *PCNA*. At the same time, an equivalent increase in the level of Cl.Caspase 3 induces cell death in CNCC, which decreases the actual population of cells required for the patterning of structures. Overall, CNCCs are unavailable for the normal patterning of frontonasal prominence in treated embryos as a result of the deleterious effects of COX-2 function disruption.

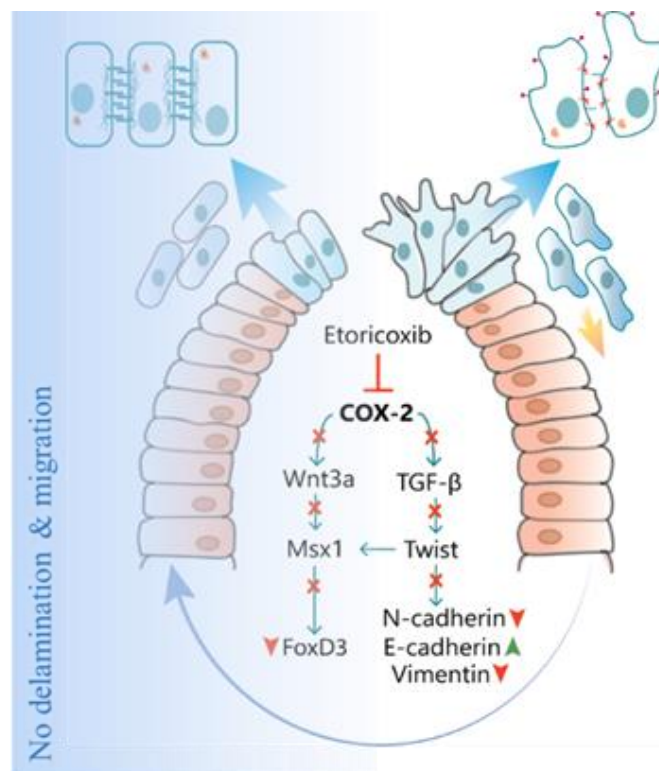


Figure 3.13: Summary Image; Inhibition of COX-2 via etoricoxib affects the regulatory molecules and hinders the process of delamination of the neural crest cells from the neural tube

Our findings suggest that COX-2, possibly via its downstream effector PGE₂, controls the temporal expression pattern of the factors responsible for CNCC formation, proliferation,

and migration (Fig 3.13). Dysregulation of cranial patterning, as observed in the present study, would cause craniofacial dysmorphism if the normal titer of COX-2 were to be altered by accidental prenatal exposure to its commonly used pharmacological inhibitors.

'The only interesting thing about vertebrates is neural crest'.

- Thorogood 1989

Tables:

Table 3.1: COX-2 activity of control and treated embryos during HH6, HH12 and HH20 stages of development of chick embryo

HH stages	Activity (nmoles/min/ml)	
	Control	Treated
HH6	1.9133 ± 0.0117	0.6474 ± 0.0011***
HH12	0.9370 ± 0.0231	0.2768 ± 0.0015***
HH20	0.7810 ± 0.0113	0.3255.0014***

Enzyme activity are expressed as Mean±SEM, n=3 with 30 eggs per group per stage; ***p≤0.001

Table 3.2: Mortality analysis of chick embryos

GROUP	HH 6	HH 12	HH 20
CONTROL	2 (1,4)	2 (1,6)	3 (2,7)
TREATMENT	10 (8,13)***	13 (8,15)***	13 (9,15)***

Mortality was observed in HH6, HH12, and HH20 stages of embryonic development in control and Etoricoxib treated groups. The values are expressed as a mode with a range in parentheses; n=3 with 30 eggs per group per stage; ***p≤0.001

Table 3.3: Transcript levels of genes responsible migration of CNCC on HH6 stage control and etoricoxib treated embryos

Gene expression	Fold change
<i>WNT3A</i>	4694.478853 ± 840.9910828*
<i>TGFB</i>	0.570743154 ± 0.510695476
<i>MSX1</i>	13.14425081 ± 1.350943522***
<i>TWIST</i>	2.042476074 ± 0.549510752
<i>CDH1</i>	0.271840406 ± 0.018177005***
<i>CDH2</i>	0.249321926 ± 0.053035819**
<i>VIM</i>	0.167340276 ± 0.000827974***
<i>PCNA</i>	0.093442309 ± 0.03684215 **
<i>CASP3</i>	0.039591223 ± 0.007778757***

Fold changes are expressed as Mean \pm SEM. Fold change values are compared with control embryos for all genes; n=30 for three technical replicates per group per stage; *p \leq 0.05, **p \leq 0.01, ***p \leq 0.001

Table 3.4: Transcript levels of genes responsible for CNCC migration on HH12 stage of development in control and etoricoxib treated chick embryos

Gene expression	Fold change
<i>WNT3A</i>	0.000583869 \pm 0.000403514***
<i>TGFB</i>	8.58354E-12 \pm 7.04672E-12***
<i>MSX1</i>	0.000216685 \pm 2.68672E-05***
<i>TWIST</i>	0.000126627 \pm 8.60444E-05***
<i>CDH1</i>	10.69343963 \pm 1.247102138**
<i>CDH2</i>	4.11549E-06 \pm 2.23463E-06***
<i>VIM</i>	0.000135061 \pm 6.76522E-05***
<i>PCNA</i>	0.000167079 \pm 0.000103949**
<i>CASP3</i>	27.52111621 \pm 3.70429533**

Fold changes are expressed as Mean \pm SEM. Fold change values are compared with control embryos for all genes; n=30 for three technical replicates per group per stage; **p \leq 0.01, ***p \leq 0.001

Table 3.5: Transcript levels of genes responsible for CNCC migration on stage HH20 control and etoricoxib treated embryos

Gene expression	Fold change
<i>WNT3A</i>	0.122468738 \pm 0.013774168**
<i>TGFB</i>	0.374790936 \pm 0.084698634**
<i>MSX1</i>	5.497035255 \pm 1.318762185
<i>TWIST</i>	2.673366093 \pm 0.474900786
<i>CDH1</i>	11.56024133 \pm 2.717506876*
<i>CDH2</i>	23.8715628 \pm 0.540268206*
<i>VIM</i>	0.146869226 \pm 0.032812497*
<i>PCNA</i>	0.175687765 \pm 0.107820407**
<i>CASP3</i>	33.6560071 \pm 3.194356841**

Fold changes are expressed as Mean \pm SEM. Fold change values are compared with control embryos for all genes; n=30 for three technical replicates per group per stage; *p \leq 0.05, **p \leq 0.01

Table 3.6: Spot densitometry analysis of the western blot bands for proteins responsible for CNCC migration on HH6, HH12 and HH20 development stages of chick embryos

Protein	Band intensity in arbitrary units	
	Control	Treatment
HH6		
E-Cadherin	57.77 ± 1.89	89.58 ± 0.70***
N-Cadherin	83.44 ± 0.22	49.72 ± 2.34***
PCNA	98.18 ± 1.03	77.45 ± 1.10***
Caspase-3	1.180 ± 0.003	1.120 ± 0.0014***
HH12		
E-Cadherin	0.24 ± 0.002	0.6 ± 0.004***
N-Cadherin	0.56 ± 0.007	0.26 ± 0.0002***
FoxD3	0.23±0.0003	0.19±0.002***
Vimentin	0.27±0.002	0.28±0.001*
PCNA	0.76 ± 0.003	0.4±0.004***
Caspase-3	1.09 ± 0.006	1.13 ± 0.003*
HH20		
E-Cadherin	45.34 ± 0.105	62.29 ± 2.307**
N-Cadherin	85.22 ± 0.982	61.60 ± 1.334***
FoxD3	57.44 ± 0.471	39.42 ± 0.071***
Vimentin	62.82 ± 0.412	50.88 ± 0.494***
PCNA	49.66 ± 2.915	38.66 ± 1.583*
Caspase-3	1.279 ± 0.134	1.099 ± 0.030

The values are expressed as Mean ± SEM; n=3 with 30 eggs per group per stage; *p≤0.05, **p≤0.01, ***p≤0.001